Rates of Homogeneous Ice Nucleation in Levitated H_2O and D_2O Droplets†

Peter Stöckel*,‡

Boehringer Ingelheim Pharma GmbH & Co. KG, Binger Str. 173, 55216 Ingelheim am Rhein, Germany

Inez M. Weidinger§

Max-Volmer-Institut für Biophysikalische Chemie, Technische Universität Berlin, Strasse des 17. Juni 135, 10623 Berlin, Germany

Helmut Baumgärtel||

Institut für Physikalische und Theoretische Chemie, Freie Universität Berlin, Takustr. 3, 14195 Berlin, Germany

Thomas Leisner⊥

Institut für Physik, Technische Universität Ilmenau, Postfach 100565, 98684 Ilmenau, Germany

Received: May 29, 2004; In Final Form: October 30, 2004

Rates of homogeneous nucleation of H_2O droplets in a temperature range from 236.37 to 237.91 K and of D_2O droplets from 241.34 to 242.33 K were measured. The single microdroplets consisted of pure H_2O or D_2O and were levitated in an electrodynamic balance. In comparison to H_2O, D_2O shows a stronger tendency to nucleate. Over the investigated temperature interval, D_2O droplets need to be supercooled less by 1.1 K compared to H_2O droplets in order to arrive at the same nucleation rate. This is in good agreement with the higher degree of intermolecular association in liquid D_2O, a fact which has been well established previously both from theory and experimental studies.

1. Introduction

Water is the most important and most intensively studied chemical compound on earth. Its phase transitions between the gaseous, liquid, and solid states have a great impact on our weather and climate.

If a sample of pure liquid water, which does not come into contact with any solid surface, is being cooled to temperatures below the melting temperature of ice, the sample can be kept nevertheless liquid for some time. This phenomenon is called supercooling. The crystallization process cannot start unless a solid icelike cluster of critical size has been formed before. Since no solid surface is present, which might act as an ice nucleus, the formation of the critical cluster is rather unlikely. The stochastic process of nucleus formation is called nucleation. We speak of heterogeneous nucleation if solid particles are involved. Otherwise, the process is called homogeneous nucleation.

The supercooled state of a liquid represents a thermodynamically metastable state. Therefore, a supercooled liquid can exist only for a finite time. The nucleation rate, $J(T)$, is proportional to the probability per time and volume of the supercooled liquid sample that crystallization of the sample will be initiated by spontaneous formation of a nucleus in the liquid. $J(T)$ is substance specific and usually a very steep function of temperature.[1]

Heavy water, D_2O, behaves very similar to H_2O, but due to the effect of isotopic substitution, a higher bond energy and a lower zero point energy of the intramolecular vibrations are observed. In comparison to H_2O, the mean cluster size in D_2O is larger at a certain temperature.[2] This phenomenon is reflected by the fact that D_2O ice exhibits a melting temperature 3.82 K higher than that of H_2O ice. The mean cluster size in D_2O is even larger than that in H_2O if we compare the two liquids at the same supercooling, $\Delta T = T^{H_2O} - T_m^{H_2O} = T^{D_2O} - T_m^{D_2O}$.[2]

The ideas briefly sketched above are the very basics of classical nucleation theory. Although the molecular structure of water is very simple, the theoretical description of the liquid's properties is a tough task, since water forms very complex molecular aggregates. Many theoretical models have been established to explain the extraordinary properties of water.[3−8] On the basis of these models, it may be possible in the future to calculate nucleation rates without the assumptions of classical nucleation theory, for example, by molecular dynamics (MD) simulations.[9] At that time, reliable experimental data will be strongly desired, enabling us to compare theory and reality.

In this paper, we present new data regarding the nucleation rates of droplets created from pure liquid H_2O or D_2O. These droplets had an average diameter of $\approx 90\ \mu$m and were levitated in a cooled electrodynamic balance.

2. Experimental Setup

Electrodynamic levitation of charged particles has been widely used for studies of atmospheric processes.[10] Our experimental setup was already described in great detail elsewhere.[11−13] In the following, we will only give a brief overview.

In Figure 1, both a vertical and a horizontal cross section through the apparatus are shown. The electrodynamic trap

† Dedicated to Erwin Biller.

* To whom correspondence should be addressed.
‡ E-mail: peter.stoeckel@web.de.
§ E-mail: inez.weidinger@tu-berlin.de.
|| E-mail: baum@chemie.fu-berlin.de.
⊥ E-mail: thomas.leisner@tu-ilmenau.de.

10.1021/jp047665y CCC: $30.25
Published on Web 02/25/2005

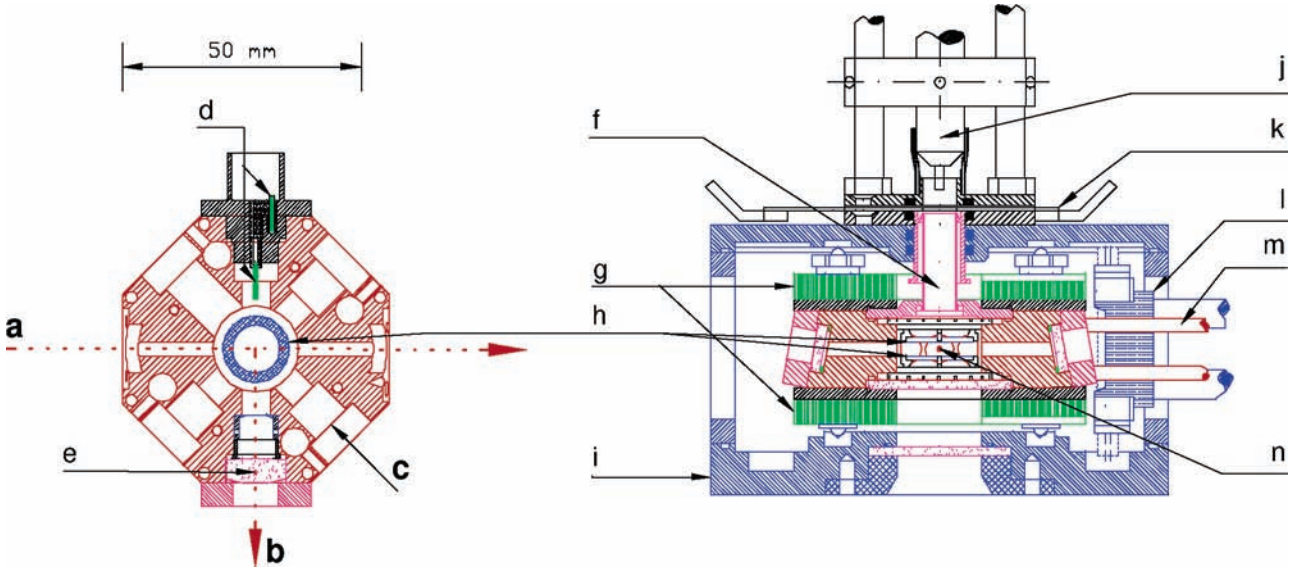

Figure 1. Horizontal (left) and vertical (right) cross section through the setup: (a) linearly polarized He−Ne laser beam; (b) observation of scattered light; (c) window for direct observation (see Figure 2); (d) Pt(100) resistance thermometers; (e) lens; (f) downspout; (g) electric heating plates; (h) ring electrodes; (i) vacuum chamber; (j) droplet generator; (k) shut-off slide; (l) cooling finger; (m) gas inlet for purging of inner trap volume; (n) levitated droplet.

consists of two ring electrodes with an inner diameter of 10 mm. These rings are arranged concentrically one above the other with a distance of 3 mm between. A harmonic alternating voltage with an amplitude of ≈ 5 kV is applied to both rings. The resulting time-dependent electric field is able to trap an electrically charged droplet. In addition, a constant potential difference of about a few 10 V is present between the rings in order to compensate the gravitational force on the droplet. The electrodes are mounted inside an octagonal trap body made from massive copper and equipped with ports for optical and electric access to the trap.

Since the nucleation rate is such a strongly temperature-dependent property, we have to pay the greatest attention to a highly precise temperature control and measurement.

The copper trap body is attached by copper fabric ribbons to a cooling finger which is flown through by liquid or cold gaseous nitrogen. To reach the desired temperature and keep it as precisely constant as possible, two flat electric heating plates, also made from copper, cover sandwichlike the top and the bottom of the trap body. An outer vacuum chamber ($p \approx 10^{-6}$ mbar) surrounds the whole setup and provides thermal insulation.

There is no way to measure the temperature directly in the center of the trap where the droplets nucleate. Mounting a sensor at that place would disturb the electric field and provoke electric breakthrough from the rings to the sensor. In addition, the supercooled droplet could come into contact with the sensor, leading to instantaneous heterogeneous nucleation and freezing. However, since the overall inner volume of our trap is rather small ($V \approx 7$ cm^3), we believe that there is practically no difference between the temperature in the center and that in the periphery of the trap. For surveillance of temperature at the latter location, we use two Pt(100) resistors. One sensor is glued into a copper flange, being in tight contact with the cooled massive copper housing. The second sensor is located directly in the gas phase, close beside the two ring electrodes. The resistance of both sensors is measured with high precision using the four-wire technique.

The calibration procedure of the setup has already been described in great detail.[11] Despite considerable efforts, we do not consider the accuracy of our absolute temperature measurement to be better than ± 0.25 K. The biggest interference comes probably from heat conduction through the connecting wires. Furthermore, we assume the temperature at the location of the droplets to be identical with the temperature measured by the sensor between the ring electrodes. However, it is possible that there is in fact a difference between these temperatures. This uncertainty also contributed to the estimated accuracy interval given above.

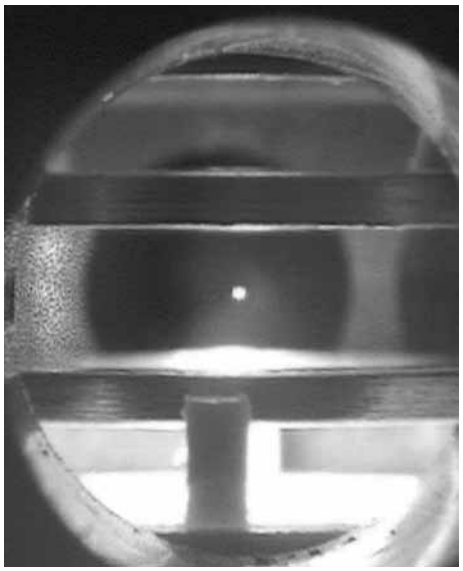

Figure 2. View into the trap along the direction c in Figure 1. In the middle between the two horizontal metal rings, the droplet can be observed as a bright spot. The droplet appears larger than it actually is ($d \approx 90$ μm). This phenomenon is mainly due to a "blooming effect" of the CCD camera chip. The free distance between the two horizontal rings is 3 mm.

It is much easier to record relative changes in temperature than to measure absolute temperatures. Our system allows to detect temperature changes with a resolution of ± 0.025 K.

The single droplets are produced at room temperature by a home-built piezoelectrically driven injector which is located above a vertical downspout. After its formation, the droplet falls

freely through this downspout into the cooled trap and becomes trapped there. After arriving in the trap, the droplet cools to ambient temperature very rapidly. It can be shown that the droplet is in thermal equilibrium with the surrounding atmosphere after 0.5 s at the latest.[11] The speed of cooling depends on the droplet diameter, of course (see the plateau for $V\,t < 3 \times 10^{-7}$ cm^3 s in Figure 5.b and its explanation in the next section).

Inside both the trap and the downspout, atmospheric pressure prevails. Prior to the beginning of the experiments, the trap is purged by cool nitrogen gas, and a very weak gas flow is usually maintained during the measurements. This is especially important in the case of D_2O.

If D_2O is in contact with humid air, it takes up H_2O readily. Subsequently, proton exchange leads to the formation of HDO. To avoid polluting, the transfer of D_2O from the sealed bottle into the injector reservoir was performed under strong exclusion of air using dry nitrogen gas for purging and shielding.

H_2O was triply distilled in a quartz-glass apparatus before usage. The D_2O was purchased from Groupe C. E. Saclay, Gif-Sur Ivette, France, and had a purity of 99.9%. Both liquids were squeezed through a Nylon filter with a 0.22 μm pore width prior to usage in order to remove solid microparticles larger than the filter pore size. We believe that after distillation and filtration our water was devoid of particles which might act as heterogeneous nuclei. If some of our droplets still had contained some, these droplets would have shown separate nucleation statistics within the ensemble of the other clean droplets. We did not observe at all such a "clustering" in the data.

The reservoir liquid inside the piezoelectric injector is kept at a constant electric potential of ≈ 1.8 kV using an electrode. When the droplet is being ejected, it becomes electrically charged. Each droplet carries about 10^5-10^6 elementary charges. Earlier experiments demonstrated that the nucleation behavior does not depend on the electric charge density on the droplets.[14]

The droplet, being levitated in the center of the trap, is illuminated by a linearly polarized He−Ne laser ($\lambda = 632.8$ nm, $P = 25$ mW). The spatial intensity distribution of the light scattered by the droplet can be described very precisely by the Mie theory.[15−18] In our experiment, an optical system consisting of lenses and a pinhole looks perpendicularly onto the direction of the laser beam and projects the light, which has been scattered by the droplet, onto a charge-coupled device (CCD) camera. The image data are transmitted with a rate of ≈ 12 frames/s to a PC and analyzed online by an algorithm based on the Mie theory. From this analysis, we gain information about the droplet diameter, d, with a time resolution of ≈ 80 ms. This procedure is subject to both random and systematic errors. We estimate our accuracy in the determination of the droplet diameter to be better than $\pm 9\%$.[11]

As long as the droplet is still liquid, it can be envisaged as an ideal sphere with optically isotropic properties and the polarization state of the light is not altered by the scattering process at this sphere. The frozen droplet, however, is not ideally spherical and optically isotropic anymore and depolarizes the light partially during scattering. This fact gives us the opportunity to detect the change in the state of aggregation of the droplet unambiguously and fast by analyzing the polarization state of the scattered light. For this purpose, two foil polarization filters with perpendicular orientation are mounted in front of the CCD camera. For more experimental details, see the literature.[11−14,19]

To determine nucleation rates, the temperature inside the trap is held at a constant value well below the melting point of ice where nucleation occurs for the large majority of droplets no later than ≈ 4 min after the injection. As long as the droplets are still liquid, they evaporate slowly. After ≈ 4 min, they have become so small that they cannot be held anymore in the trap.

While there is permanent evaporation of water from the droplet's surface, the droplet loses steadily heat of evaporation and its temperature falls below the temperature of the environment. The steady state is reached when the heat flux from the environment into the droplet compensates the loss of evaporation heat. On the basis of the conditions in our experiment, we calculated the droplet temperature to lie ≈ 0.2 K below the temperature of the environment of the droplet which is the temperature we actually measure.[11] For reasons of simplicity and comparability, we do not take this permanent temperature shift into consideration in the following. However, one should keep this issue in mind, since it is obviously not negligible.

Several thousands of droplets were injected consecutively. The time expired between the injection and the freezing event was recorded for each droplet. After freezing had occurred, the frequency of the alternate voltage at the ring electrodes was lowered for a short moment so that the ice particle fell down to the bottom window of the trap. Afterward, the cycle started with a new droplet again.

3. Results

The freezing of supercooled water is a first-order phase transition.[20] The decay of the number, N_u, of unfrozen droplets in a cloud of N_0 frozen or supercooled water particles can then be considered as a reaction of first-order kinetics,[21,22] following the equation

$$\ln \frac{N_u}{N_0} = -J\,(T)\,V\,t \qquad (1)$$

In analogy to true chemical reactions, the nucleation rate, J, is a rate constant, giving the (average) number of nucleation events per volume and time. We are well aware about the argument going on in the literature on the question of whether nucleation of ice in supercooled droplets might be initiated on the surface of the droplets rather than in the bulk volume.[23,24] The argumentation is based upon an analysis of numerous experimental data for nucleation rates in droplets. As a matter of fact, there is a competition between both nucleation mechanisms, depending on the size of the droplets and the nature of their interface.

We examined our data very critically with respect to surface nucleation but could not find any hint for this mechanism being involved. The results of a recently conducted experimental in-depth study concerning this issue have been published very recently.[25] In the atmosphere, water droplets that directly freeze into ice are much smaller than ours, and therefore, our studies cannot contribute to the argument of whether in the atmosphere homogeneous freezing of droplets occurs in the volume or on the surface.

If the volume of the droplets were constant in time, the number of liquid droplets, N_u, would decrease exponentially with rising time. However, since the volume of the supercooled droplets is not constant but rather a function of time due to evaporation, we change over from the t coordinate to the $V\,t$ coordinate. Now N_u decays exponentially with rising $V\,t$.

In parts a and b of Figure 3, all nucleation times measured with H_2O and D_2O droplets, respectively, are shown over the

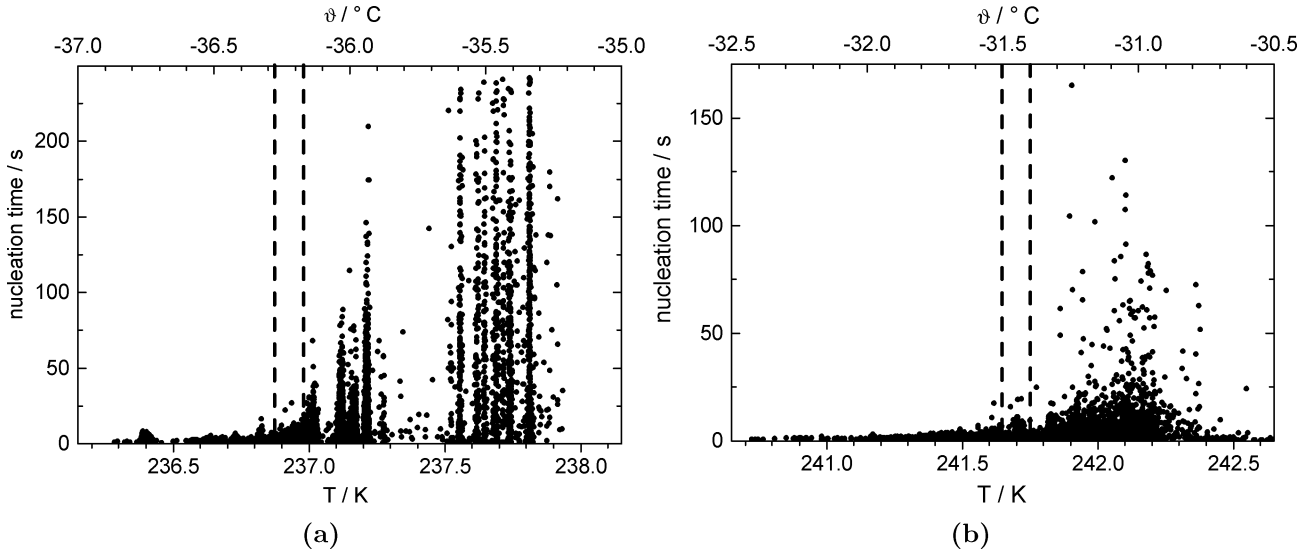

Figure 3. Nucleation time vs the temperature at which nucleation occurred. The bins confined by the vertical dashed lines contain those points which contributed to Figures 4 and 5: (a) data of all 8737 H_2O droplets under investigation; (b) nucleation of 7204 D_2O droplets was observed.

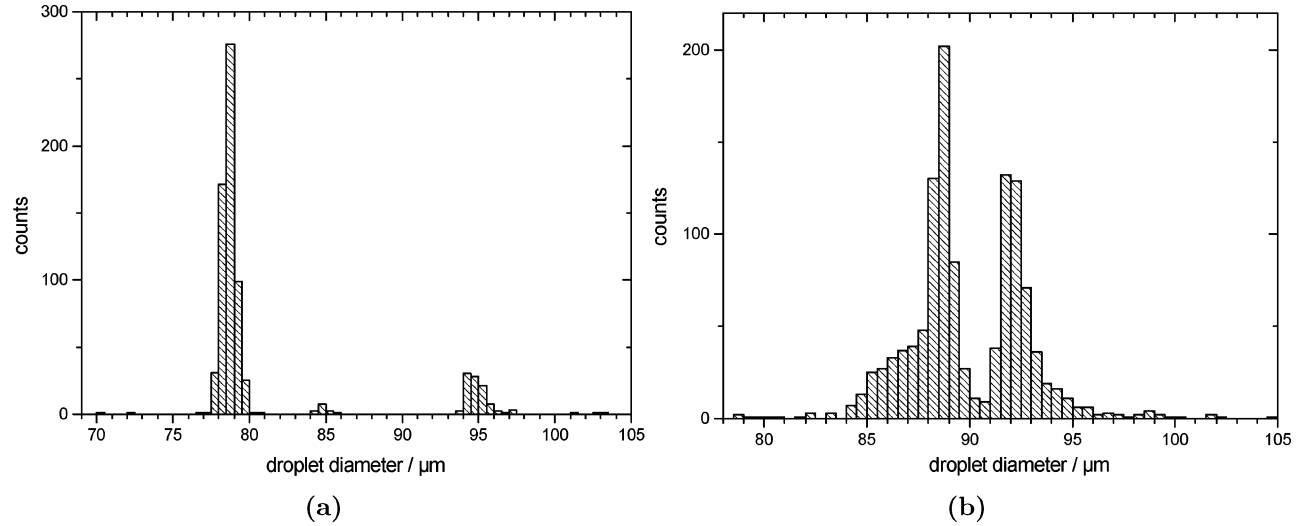

Figure 4. Histograms showing the number of droplets over their diameter at the instant of freezing. Only those droplets inside the bins confined by dashed lines in Figure 3 have been considered: (a) 717 droplets, mean freezing diameter 81.0 μm, standard deviation 5.7 μm; (b) 1194 droplets, mean freezing diameter 89.9 μm, standard deviation 3.0 μm.

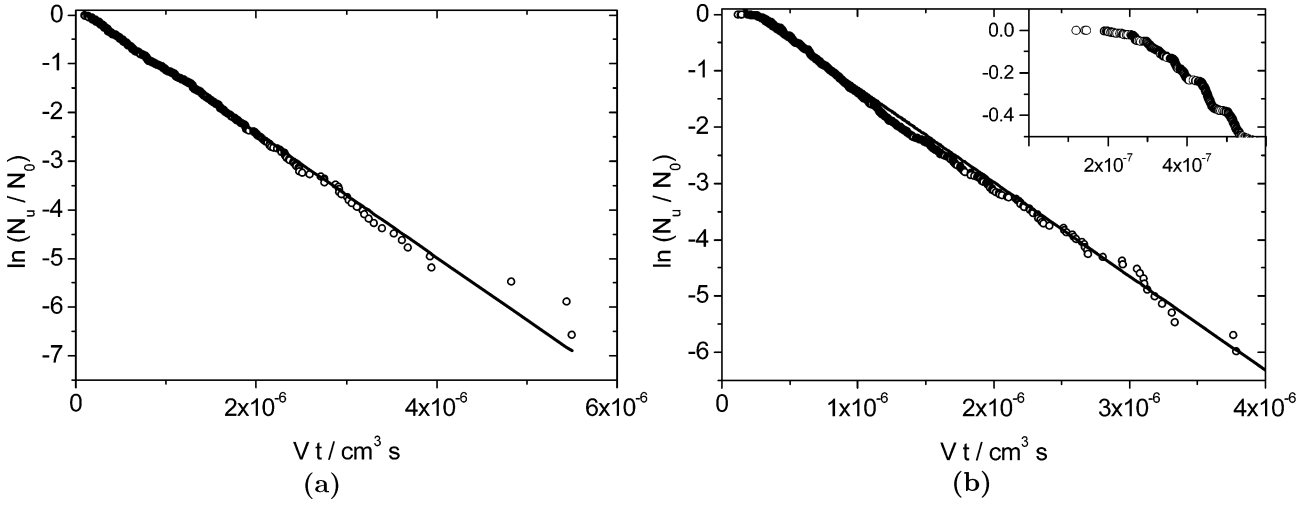

Figure 5. $\ln(N_u / N_0)$ plotted vs $V\,t$ for the droplets inside the intervals in Figure 3. N_u = number of unfrozen droplets at "volume-scaled" instant $V\,t$. N_0 = number of all droplets lying inside the temperature interval under consideration. V = droplet volume at instant of freezing: (a) plot for 717 H_2O droplets which nucleated between $T = 236.88$ K and $T = 236.98$ K, arithmetic mean over all freezing temperatures $\overline{T_i} = 236.94$ K; (b) plot for 1194 D_2O droplets which nucleated between $T = 241.65$ K and $T = 241.75$ K, arithmetic mean over all freezing temperatures $\overline{T_i} = 241.71$ K.

temperature at which the observation took place. Because we need a not too small number of points for each particular temperature, we discretize the temperature coordinate by creating temperature intervals of 0.1 K width and consider for the subsequent evaluation all those points lying inside a particular interval. Each interval, j, is characterized by a mean temperature, T_j, which has been calculated by averaging the temperature over all points inside the interval.

In both parts a and b of Figure 3, there is one of those intervals marked by two vertical dashed lines. For these intervals, Figure 4 shows the frequency distribution of droplet diameters at the instant of freezing. In both cases, the distribution seems to be somehow bimodal. This is caused by the fact that, in continuous operation over many hours or days, our droplet generators are not always producing droplets of the same size but rather tend to switch randomly between two or sometimes even more modes of operation from time to time.

To determine J for interval j, we form for each droplet, i, the product of its volume, V_{ij}, at the instant of freezing and its nucleation time, t_{ij}. Afterward, we order the droplets with regard to the falling product $V_{ij}\,t_{ij}$ and obtain $N_u(V_{ij}\,t_{ij})$ by identifying N_u with the position of the particular droplet in the ordered row, starting with $N_u = 1$ for the second-largest product $V_{1j}\,t_{1j}$. Thus, N_u can still be considered as the number of unfrozen droplets, namely, in the "volume-scaled time coordinate".

Plotting the logarithm on the left side of (1) versus $V\,t$, a straight line is obtained indeed (see Figure 5), and the nucleation rate, J, is equal to the negative slope of this straight line. While the mean diameter of all droplets under consideration in Figure 5a was 81.0 μm, the droplets in Figure 5b were somewhat larger ($\bar{d} = 89.9\ \mu$m). Thus, the D_2O droplets cooled somewhat slower after injection into the trap. This led to a slower increase of the nucleation rate after injection, resulting in a small plateau for $V\,t < 3 \times 10^{-7}$ cm^3 s.

The straight lines in Figure 5 are especially remarkable if we remember the bimodal frequency distribution of diameters in Figure 4. If we encountered surface nucleation rather than volume nucleation in a substantial fraction of droplets, we would not expect a simple exponential decay of N_u with increasing $V\,t$.

Our experiments were carried out in the temperature range between 236.37 and 237.91 K for H_2O droplets and 241.34 and 242.33 K for D_2O droplets. In these two temperature intervals, the nucleation rates of both liquids are of the same order of magnitude (see Figure 6), so that the mean nucleation time of the droplets is also of the same order of magnitude for both liquids under consideration. If we want to study the nucleation statistics of the droplets using our experimental setup, we must make sure that most droplets nucleate no earlier than about a few tenths of a second and no later than $\approx$ 4 min after their injection into the trap. These two constraints are caused by the limited frequency (12 Hz) of our image acquisition system on one hand and by the permanent evaporation of the supercooled droplets in the trap on the other hand. We have tried to broaden the accessible temperature range a little bit by using larger droplets at higher temperatures and smaller droplets at lower temperatures, but nevertheless, the accessible interval remained rather narrow. It was not possible to make the two intervals overlap.

Repeating the procedure described above for all temperature bins yields a set of nucleation rates at different temperatures which can be compared with the rates determined by other groups (see Figure 6).

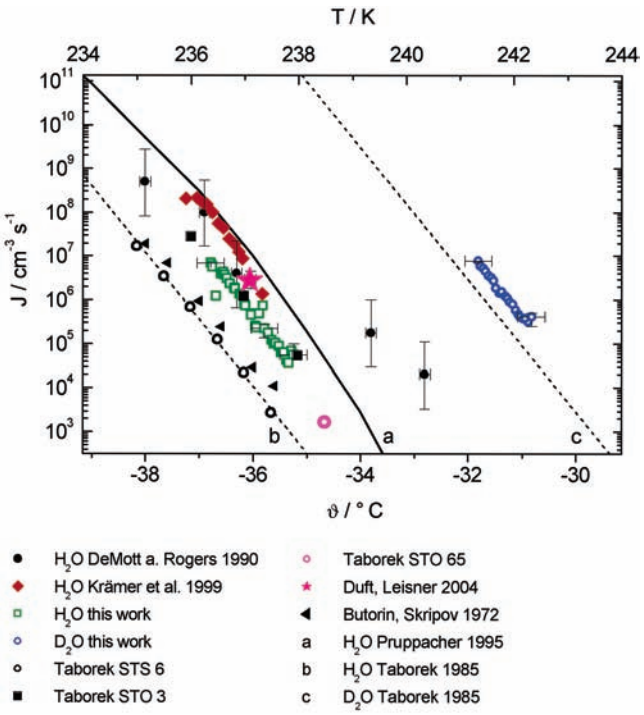

Figure 6. Nucleation rates of supercooled H_2O and D_2O as measured in this work and by other authors.

The nucleation rates of H_2O published by Krämer et al. in 1999[14] were measured in an electrodynamic balance as well, whereas DeMott and Rogers studied homogeneous nucleation in diluted aqueous salt solution droplets using an aerosol cloud chamber.[26]

Curve a in Figure 6 was obtained by Pruppacher,[1] when he fitted the expression for J derived by classical nucleation theory to all data which had been published until 1995.

Curves b and c in Figure 6 show linear functions obtained by Taborek from experimental data.[27] He observed ice nucleation in supercooled emulsions of water in petroleum jelly. In the case of H_2O, he used either sorbitan tristearate (STS) or sorbitan trioleate (STO) as the surfactant. In the case of D_2O, only STS was employed. For his linear approximations, Taborek only used the STS data because, as he states, the STO data exhibited hints for favored surface nucleation at the surfactant layer. Obviously, Taborek's STS curves are somewhat shifted against the data of other authors toward lower temperatures. This discrepancy, which is corroborated by our data not only for H_2O but also for D_2O, was already discussed by Pruppacher.[1] He suggested that the STS might have been dissolved in tiny amounts in the water, provoking an inhibiting effect on the nucleation in the bulk water of the droplets.

However, if STS indeed mixed in tiny amounts with water and inhibited nucleation, we would expect to observe a similar decrease of J for the D_2O−STS emulsions. Instead, this shift appears actually to be much smaller than in the case of H_2O−STS. This might have been caused by a smaller solubility of STS in D_2O.

Butorin and Skripov[28] used a method very similar to that of Taborek. They immersed single water droplets with diameters between 20 and 500 μm in a "vacuum oil" and observed the freezing event by means of differential thermal analysis.

Experiments using emulsions will always keep being very subtle, not only with respect to an interaction between the two

phases at the droplet interface but also with respect to a possible marginal solubility of the nonaqueous phase in water.

There is still another puzzling feature in Figure 6. Since DeMott and Rogers used water droplets in which small amounts of inorganic salts were dissolved, we would expect their rates to deviate downward at a certain temperature, similarly as the Taborek STS data does. The fact that this is not the case may perhaps be explained by assuming that surface nucleation played a role. DeMott and Rogers used rather small droplets with a diameter from 3 to 7 μm.

Eventually, we have to address the possibility not that Taborek's data might lie too low but rather the data stemming from experiments in electrodynamic traps might be shifted upward due to the influence of the electric fields in the trap on the structure of the liquid water molecule network. However, from a theoretical point of view, such an influence is rather unlikely as long as nucleation takes place in the bulk volume and not on the surface. Pure liquid water is not a good electric conductor but still is one. Hence, the positive electric charges on the droplet, that is, the excess hydronium ions, distribute themselves homogeneously in a very thin surface layer on the droplet. The charge density on the droplet surface will be altered periodically by the electric fields in the trap, but in the interior bulk volume of the droplets, there is essentially no excess charge and therefore no electric field at all. Thus, the droplet can be looked at as a field-free Faraday cage. Only if nucleation happened in the very thin charged surface layer of the droplet, we would expect to see an influence of the external electric field on nucleation. In our experiments, we could not observe any relationship between the voltage applied to the electrodes of the trap and the nucleation statistics of the droplets.

The slope d lg$J$/dT of all the data and curves presented in Figure 6 is very similar. Only the results of DeMott and Rogers show a somewhat weaker temperature dependence. Especially the two points at higher temperatures seem not to fit into the picture. In these rates, both homogeneous and heterogeneous nucleation were probably involved, as the authors suggest themselves.[26]

Until now, the work of Taborek[27] is the only one in the literature regarding rates of homogeneous nucleation of ice in liquid D_2O.

At this point, we wish to explain the inconsistency which apparently exists between the nucleation rates published in the present paper and the rates published earlier by our group.[12] The former results, which we obtained in an electrodynamic trap using pure water droplets as well, are shifted to higher temperatures and do not form a single line with our newer nucleation rates. In the meanwhile, we have reconducted and extended our studies and could not reproduce our previous data. We believe now that our initial measurements were impaired by experimental problems in temperature measurement and droplet volume determination.

Within the investigated temperature intervals (236.37−237.91 K for H_2O and 241.34−242.33 K for D_2O), our data can be approximated very well by the following linear functions:

$$\lg(J_{H_2O}/(\mathrm{cm}^{-3}\,\mathrm{s}^{-1})) = (-1.46 \pm 0.07)(T - T_m)/\mathrm{K} - 46.98 \pm 2.3 \qquad \text{for } H_2O$$

and

$$\lg(J_{D_2O}/(\mathrm{cm}^{-3}\,\mathrm{s}^{-1})) = (-1.45 \pm 0.05)(T - T_m)/\mathrm{K} - 44.87 \pm 1.7 \qquad \text{for } D_2O$$

If we want to elucidate the influence of isotopic substitution on homogeneous nucleation, we must not directly compare the nucleation rates of H_2O and D_2O with respect to absolute temperature. There is a difference, $T_m^{D_2O} - T_m^{H_2O} = 3.82$ K, in the melting temperatures of the two liquids, and it is probably reasonable to compare the nucleation behavior at the same supercooling, $\Delta T = T^{H_2O} - T_m^{H_2O} = T^{D_2O} - T_m{}^{D_2O}$, rather than at the same absolute temperature. This has been done in Figure 7.

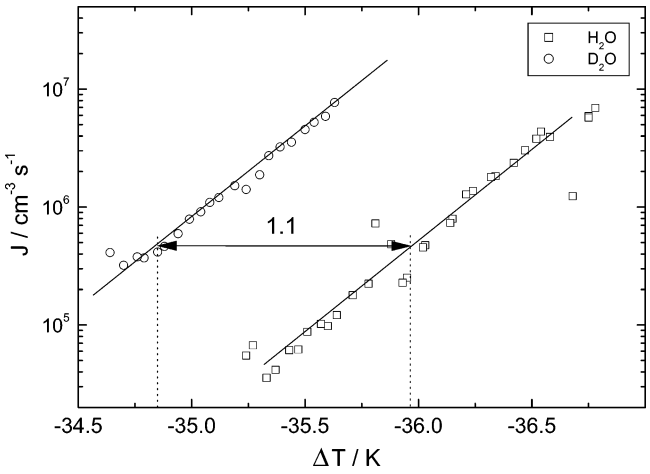

Figure 7. Nucleation rates of H_2O and D_2O as measured in this work with regard to supercooling, $\Delta T = T^{H_2O} - T_m^{H_2O} = T^{D_2O} - T_m^{D_2O}$.

While the slope d lg$J$/dT in Figure 7 is practically the same for both liquids, the two lines are shifted against each other. In comparison to H_2O, the nucleation rate in D_2O reaches the same magnitude already at a supercooling which is 1.1 K weaker than that of H_2O. Apparently, heavy water shows a higher tendency to nucleate than normal water. This observation may support the assumption that the average cluster size in equally supercooled D_2O is larger than that in H_2O, which can be inferred from earlier theoretical studies[2]. It is, however, an interesting fact that these differences between H_2O and D_2O seem not to exist in the case of the nucleation of liquid droplets in supersaturated vapors.[29]

To make the physical behavior of the two supercooled liquids comparable, there are convincing arguments for alternative shifts of the temperature scales. Vedamuthu et al.[30] suggest to shift the temperature scale for H_2O upward by 7.2 K which is the difference between the temperatures of maximal density of both liquids. They point out that this transformation would cause the structural properties of the two liquids to be nearly identical over a fairly wide range of temperature, so that—in their view—any properties that depend solely on the structure of the liquid should be equal at the same transformed temperature. According to them, this is not the case for the melting and boiling points of H_2O and D_2O because they depend not only on the structure of the liquid itself but also on the thermodynamics of the solid or gaseous phase, respectively.

If we compare the nucleation rates of the two liquids with regard to "density-coherent" temperatures, the picture sketched above turns over. Now, H_2O seems to be the liquid which nucleates easier. It reaches a particular nucleation rate already at a temperature 2.3 K above the temperature which is necessary to have the D_2O droplets nucleating with the same rate.

It becomes obvious that neither of these two strategies for temperature transformation make the nucleation behavior of the two liquids coincide indeed. This interesting observation should definitely be discussed further in future works.

4. Summary

In this paper, we reported on experiments with strongly supercooled droplets of H_2O and D_2O. These droplets were levitated in an electrodynamic balance in order to exclude heterogeneous nucleation through solid surfaces. We studied the statistics of homogeneous nucleation in ensembles comprising several thousands of droplets. The collected data allowed us to calculate the nucleation rate at different temperatures with high precision. In the case of D_2O, the presented data is the first one of its kind in the literature.

A linear dependence between $\lg(J/(\mathrm{cm}^{-3}\ \mathrm{s}^{-1}))$ and the supercooling ΔT was found. Light and heavy water exhibited the same slope, $\mathrm{d}\lg(J/(\mathrm{cm}^{-3}\ \mathrm{s}^{-1}))/\mathrm{d}T$. However, the D_2O droplets showed a certain nucleation rate already at a supercooling which was 1.1 K weaker than that of the H_2O droplets. This observation corresponds to the larger cluster sizes that are predicted for liquid D_2O in comparison to H_2O at comparable temperatures.

With our results, we hope to contribute to the ongoing scientific efforts toward a more thorough understanding of the structural peculiarities of liquid water and the homogeneous nucleation of ice therein.

Acknowledgment. We are indebted to E. Biller for continuous and vital technical support. Furthermore, we wish to thank H. Vortisch for discussions about nucleation theory and assistance with data processing. Financial support from the Deutsche Forschungsgemeinschaft (DFG) and from Fonds der Chemischen Industrie is gratefully acknowledged.

References and Notes

(1) Pruppacher, H. R. *J. Atmos. Sci.* **1995**, *52* (11), 1924.
(2) Némethy, G.; Scheraga, H. A. *J. Chem. Phys.* **1964**, *41*, 680.
(3) Eisenberg, D.; Kauzmann, W. *The Structure and Properties of Water*; Oxford Clarendon Press: Oxford, U.K., 1969.
(4) Franks, F., Ed. *Water—a comprehensive treatise*; Plenum Press: New York, London, 1972.
(5) Fletcher, N. H. *The Chemical Physics of Ice*; Cambridge University Press: London, 1970.
(6) Pruppacher, H. R.; Klett, J. D. *Microphysics of Clouds and Precipitation*; Kluwer Academic Publishers: Dordrecht, The Netherlands, 1997.
(7) Ludwig, R. *Angew. Chem.* **2001**, *113*, 1856−1876.
(8) Lock, G. S. H. *The Growth and Decay of Ice*; Cambridge University Press: New York, 1990.
(9) Matsumoto, M.; Saito, S.; Ohmine, I. *Nature* **2002**, *416*, 409−413.
(10) Davis, D. J. *Aerosol Sci. Technol.* **1997**, *26*, 212−254, P3−2.
(11) Stöckel, P. *Homogene Nukleation in levitierten Tröpfchen aus stark unterkühltem H_2O und D_2O*. Ph.D. Thesis, Freie Universität Berlin, 2001 (http://www.diss.fu-berlin.de/2002/23/).
(12) Stöckel, P.; Vortisch, H.; Leisner, T.; Baumgärtel, H. *J. Mol. Liq.* **2002**, *96*−*97*, 153−175.
(13) Weidinger, I.; Klein, J.; Stöckel, P.; Baumgärtel, H.; Leisner, T. *J. Phys. Chem. B* **2003**, *107*, 3636.
(14) Krämer, B.; Hübner, O.; Vortisch, H.; Leisner, T.; Schwell, M.; Ruehl, E.; Baumgärtel, H. *J. Chem. Phys.* **1999**, *111* (14), 6521.
(15) Mie, G. *Ann. Phys.* **1908**, *25*, 377−455.
(16) Bohren, C. F.; Huffman, D. R. *Absorption and Scattering of Light by Small Particles*; John Wiley and Sons: New York, 1983.
(17) Kerker, M. *The scattering of light*; Academic Press: Oxford, U.K., 1969.
(18) Barber, P. W.; Chang, R. K. *Optical Effects Associated with Small Particles*; World Scientific: Singapore, 1988.
(19) Vortisch, H.; Krämer, B.; Weidinger, I.; Wöste, L.; Leisner, T.; Schwell, M.; Baumgärtel, H.; Rühl, E. *Phys. Chem. Chem. Phys.* **2000**, *2*, 1407.
(20) Ehrenfest, P. *Proc. K. Ned. Akad.* **1933**, *36* (Suppl. 75b), 153.
(21) Koop, T.; Luo, B.; Biermann, U. M.; Crutzen, P. J.; Peter, T. *J. Phys. Chem. A* **1997**, *101*, 1117−1133.
(22) Krämer, B.; Schwell, M.; Hübner, O.; Vortisch, H.; Leisner, T.; Rühl, E.; Baumgärtel, H.; Wöste, L. *Ber. Bunsen-Ges. Phys. Chem.* **1996**, *100*, 1911−1914.
(23) Tabazadeh, A.; Djikaev, Y. S.; Reiss, H. *Proc. Natl. Acad. Sci. U.S.A.* **2002**, *99*, 15873−15878 (http://www.pnas.org/cgi/doi/10.1073/pnas.252640699).
(24) Kay, J. E.; Tsemekhman, V.; Larson, B.; Baker, M.; Swanson, B. *Atmos. Chem. Phys.* **2003**, *3*, 1439−1443 (www.atmos-chem-phys.org/acp/3/1439/).
(25) Duft, D.; Leisner, T. *Atmos. Chem. Phys. Discuss.* **2004**, *4*, 3077−3088 (www.atmos-chem-phys.org/acpd/4/3077/).
(26) DeMott, P. J.; Rogers, D. C. *J. Atmos. Sci.* **1990**, *47*, 1056−1064.
(27) Taborek, P. *Phys. Rev. B* **1985**, *32*, 5902.
(28) Butorin, G. T.; Skripov, V. P. *Sov. Phys. Crystallogr.* **1972**, *17* (2), 322.
(29) Wölk, J.; Strey, R. *J. Phys. Chem. B* **2001**, *105*, 11683−11701.
(30) Vedamuthu, M.; Singh, S.; Robinson, G. W. *J. Phys. Chem.* **1996**, *100*, 3825−3827.